PNAS
www.pnas.org

Supplementary Information for

Abscisic acid-independent stomatal CO_2 signal transduction pathway and convergence of CO_2 and ABA signaling downstream of OST1 Kinase

Po-Kai Hsu, Yohei Takahashi, Shintaro Munemasa, Ebe Merilo, Kristiina Laanemets, Rainer Waadt, Dianne Pater, Hannes Kollist, and Julian I. Schroeder

Corresponding author: Julian I. Schroeder
Email: jischroeder@ucsd.edu

This PDF file includes:

www.pnas.org/cgi/doi/10.1073/pnas.1809204115

Supplementary Materials and Methods

Analyses of ABA Content in Rosettes.

Plants were grown under well-watered conditions for five weeks. Rosette leaves were weighed and frozen in Eppendorf tubes in liquid nitrogen. Tissues were grinded using 2.3 mm chrome steel beads using a Retsch Mixer Mill MM 400. ABA was isolated and determined according to a protocol (1) using Phytodetek Immunoassay Kit for ABA (PDK 09347/0096, Agdia, Inc., Elkhart, IN, USA).

Stomatal Index and Stomatal Density Analyses.

The eighth true leaves of 5-week-old plants grown under well-watered conditions were prepare for microscopy imaging according to a previous protocol (2). Four images (two from both sides of the mid-vein, in the middle of the leaf) of the abaxial side of the leaf were taken. Stomata number and pavement cell number in each image were manually counted using Fiji (3). Stomatal index = percentage of epidermal cells that are stomata, as calculated by 100% × (number of stomata) / (number of stomata + number of pavement cells); Stomatal density = number of stomata per mm^2.

ABA Reporter Analyses of Stress Responses.

Plants were grown on vertical plates in half-strength MS medium and 1% sucrose solidified by 0.8% phytoagar (A20300, RPI, Corp., Mount Prospect, IL, USA) at pH 5.8. For salt and ABA experiments, 14-day-old *pGC1::ABAleon2.15* seedlings were transferred to half-strength MS medium plates containing 0.02% EtOH as control, 140 mM NaCl, or 20 μM ABA. For low water potential experiments, medium plates were prepared and water potentials of media were estimated according to a previous report (4). Sixteen-day-old *pGC1::ABAleon2.15* or *pRAB18::GFP* plants were transferred to half-strength MS medium plates (-0.31 MPa) or low water potential medium plates (-0.76 MPa) generated by PEG-8000 infusion.

Fluorescence emission ratios of ABAleon2.15 in guard cells were analyzed 4 hours after the indicated treatments. The third to fifth true leaves from three plants were blended about 10 sec four times in 200 mL deionized water and leaf epidermal tissues were collected through a 100 μm nylon mesh (Millipore, Billerica, MA) and mounted on a microscope slide for imaging as describe previously (5) using 150 ms exposures to reduce bleaching of fluorescence proteins. Experiments were performed in at least triplicate and ≥ 30 guard cell pairs were analyzed in each experiment.

GFP fluorescence signals in leaves of *pRAB18::GFP* transgenic plants were observed after treatment with different water potential media for 9 hr. The third youngest leaf of each individual plant was detached and mounted on a microscope slide with deionized water for imaging. GFP signals were observed and images were captured using a custom-assembled spinning disk confocal microscope system described previously (5). Images were processed and analyzed using Fiji (3).

In-Gel Kinase Assays Performed with Mixture of Mesophyll and Guard Cell Protoplasts

To examine the effect of mesophyll cells on guard cell OST1/SnRK2.6 activation, mesophyll and guard cell protoplasts were prepared in parallel on the same day. MCPs were isolated as previously reported (6) from Col-0. GCPs were isolated from transgenic

Arabidopsis expressing *OST1-HF* under the control of the *pUBQ10* promoter in the *ost1-3* background (*pUBQ10::OST1-HF/ost1-3*) (7). 30 µg protein of GCPs and when indicated 60 µg protein of MCPs were suspended in reaction buffer (5 mM MES-KOH pH 6.0, 10 mM KCl, 1 mM $CaCl_2$ and 0.4 M mannitol) and put on ice overnight in 1.5 mL tubes. On the following day, these tubes were put on the lab bench at room temperature for 30 min, and the supernatants were removed. Protoplasts were treated with CO_2 for 15 min by addition of CO_2-equilibrated buffer and then harvested by centrifugation. In-gel kinase assays were performed as described in the main text of this report. CO_2-equilibrated buffer was prepared by prior aeration with 0 or 5% CO_2 containing air for 15 min and the pH was adjusted to 6.0 with KOH. Slight modifications in one experiment included CO_2-bubbling during the protoplast incubation instead of prior aeration. Wild type GCPs were used in two experiments with mesophyll protoplasts added and also showed no OST1/SnRK2.6 activation. For ABA treatments as an OST1/SnRK2.6 activation control, 20 µg protein of GCPs were treated with 10 µM ABA or 0.25% EtOH for 15 min.

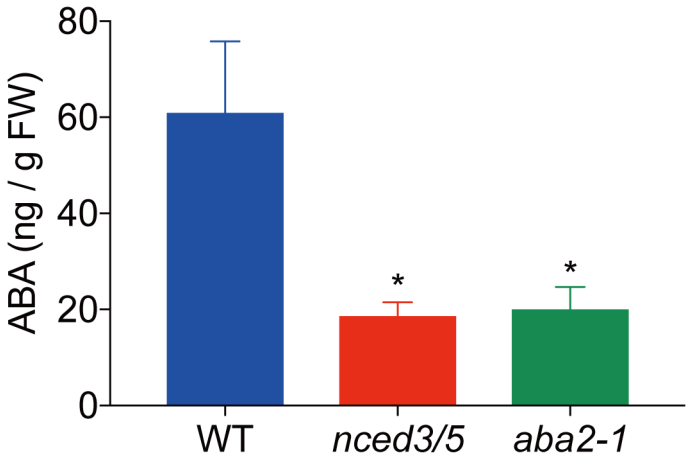

Fig. S1. Measurement of ABA content in rosettes of wild-type, *nced3/nced5* double mutant, and *aba2-1* mutant plants.
ABA concentrations in whole rosettes of wild-type, *nced3/nced5* doule mutant, and *aba2-1* mutant plants were determined using an enzyme immunoassay (Phytodetek). n = 6 plants for WT, n = 6 plants for *nced3/nced5*, and n = 5 for *aba2-1*. Data represent mean ± SEM. * $P < 0.05$ as analyzed by one-way ANOVA followed by a Dunnett's test compared to WT control.

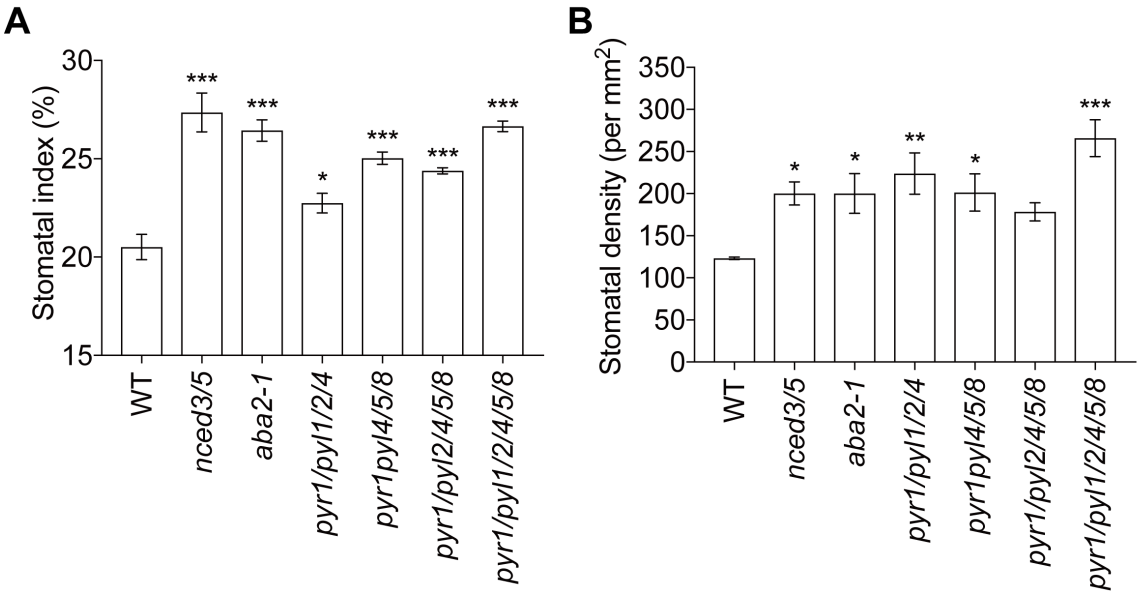

Fig. S2. ABA biosynthesis and ABA receptor mutants have higher stomatal index and stomatal density compared to wild-type.

Stomatal index and stomatal density in leaf 8 of Col-0 (WT) and indicated ABA biosynthesis and ABA receptor mutant plants were measured. Four images were analyzed in each leaf. n = 4 leaves from different plants from each genotype. * $P < 0.05$, ** $P < 0.01$, *** $P < 0.001$ as analyzed by one-way ANOVA followed by a Dunnett's test compared to WT control.

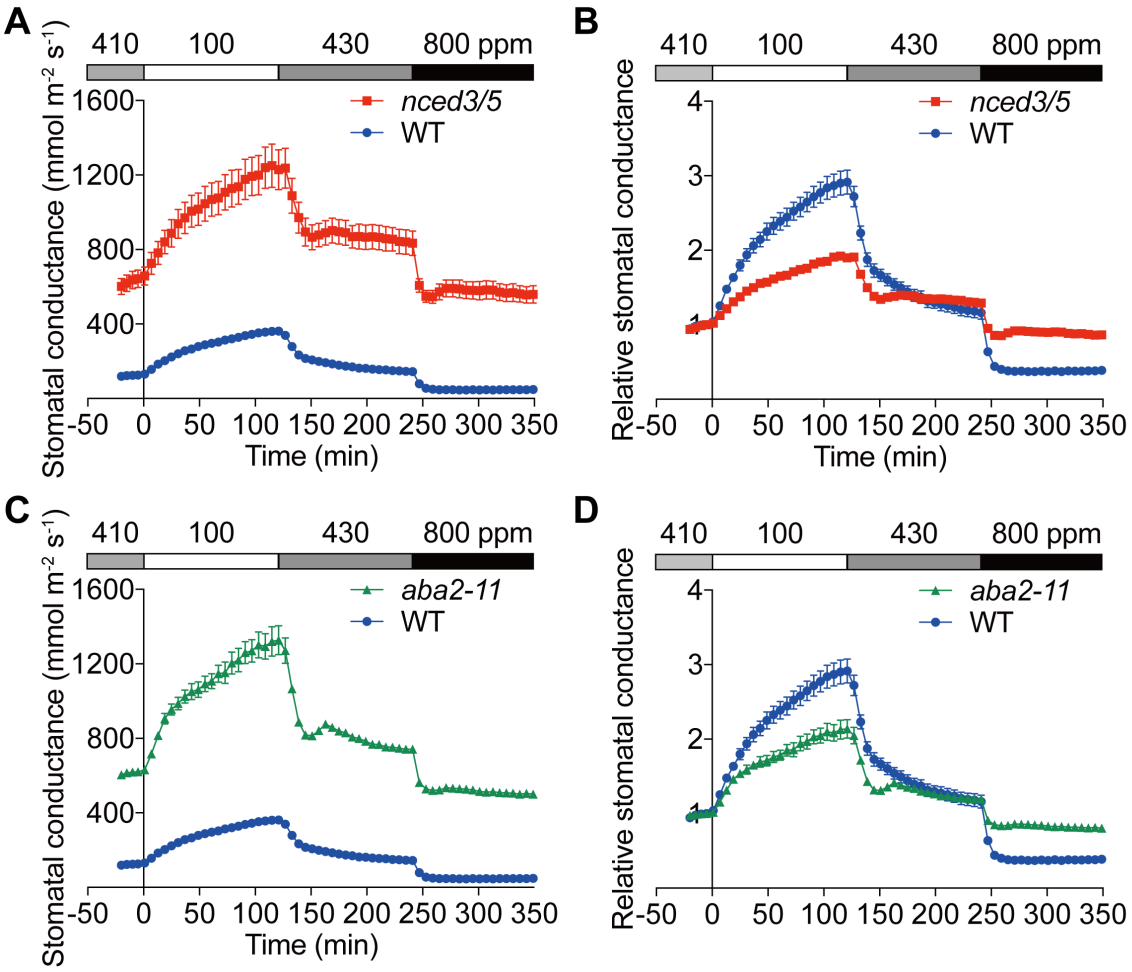

Fig. S3. Measurement of stomatal CO_2 responses in intact whole *Arabidopsis* plants. Intact whole plant gas exchange analyses conducted in *nced3/nced5* double mutant plants *(A* and *B)* and *aba2-11* mutant plants *(C* and *D)*. Absolute stomatal conductances are shown in *A* and *C*. The corresponding normalized stomatal conductances are shown in *B* and *D*. Wild-type controls are the same, because mutants and WT were analyzed in parallel. n = 7 plants for WT, n = 7 plants for *nced3/nced5*, and n = 5 for *aba2-11*. Data represent mean ± SEM.

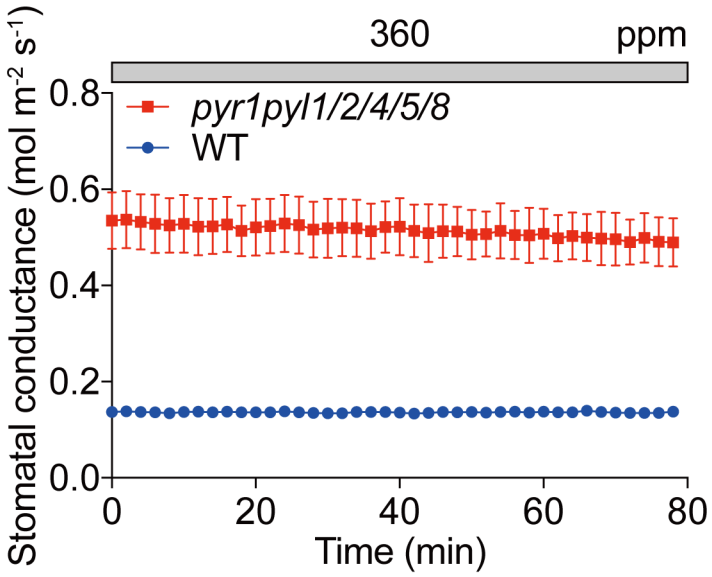

Fig S4. Stomatal conductances in wild-type and *pyr1/pyl1/pyl2/pyl4/pyl5/pyl8* hextuple mutant recorded at continuous 360 ppm ambient CO_2.
Time-resolved stomatal conductances in Col-0 (WT) and *pyr1/pyl1/pyl2/pyl4/pyl5/pyl8* (*rcar3/8/10/11/12/14*) hextuple mutant (*pyr1/pyl1/2/4/5/8*) leaves at 360ppm CO_2. n = 3 plants for each genotype. Data represent mean ± SEM.

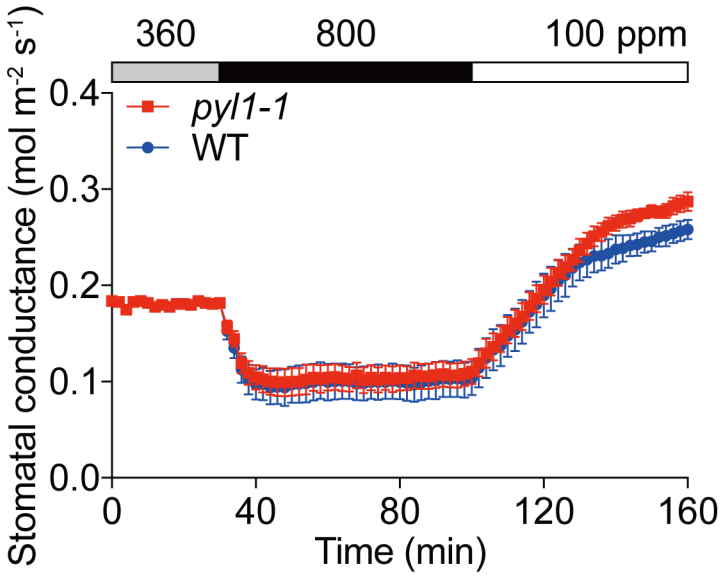

Fig. S5. Stomatal CO_2 response in *pyl1-1* mutant is similar to wild-type.
Time-resolved stomatal conductance responses to changes in ambient [CO_2] in the Col-0 (WT) and *pyl1-1* mutant. Ambient CO_2 concentrations are shown on the top. n = 5 plants for each genotype. Data represent mean ± SEM.

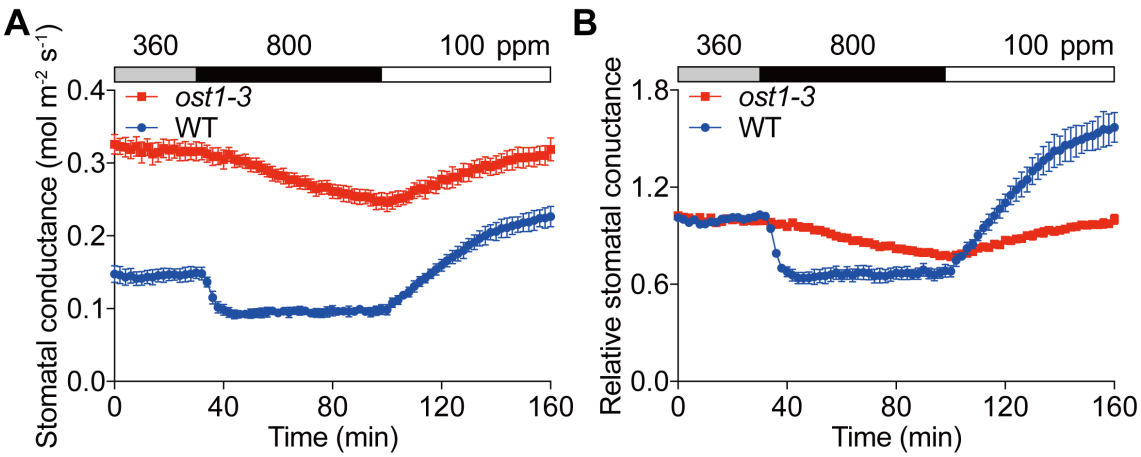

Fig. S6. Elevated CO_2-triggered stomatal closure is slowed in *ost1-3* mutant leaves. Time-resolved stomatal conductance responses to changes in ambient [CO_2] in the Col-0 (WT) and *ost1-3* mutant. Ambient CO_2 concentrations are shown on the top of traces. *(A)* Absolute average stomatal conductances of WT and *ost1-3* mutant leaves. *(B)* The corresponding relative stomatal conductance responses shown in *A* normalized to average values at 360 ppm. n = 4 plants for each genotype. Data represent mean ± SEM.

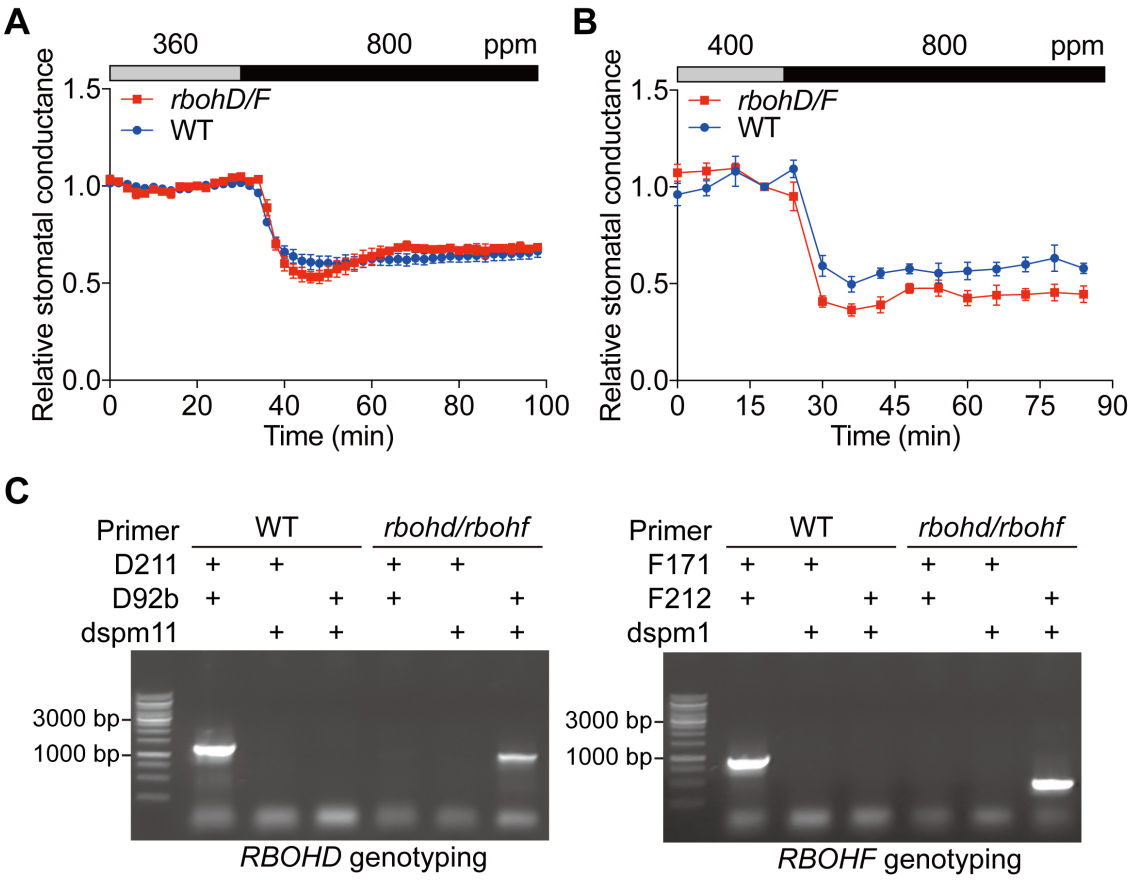

Fig. S7. Stomata in *rbohD/rbohF* double mutant leaves respond normally to elevated CO_2.

Time-resolved stomatal conductance responses to increases in [CO_2] in Col-0 (WT) and *rbohD/rbohF* double mutant (*rbohD/F*) plants. The imposed ambient CO_2 concentrations are shown on top of the data traces in each panel. *(A)* Relative stomatal conductance of WT and *rbohD/rbohF* double mutant leaves. Data represent mean ± SEM. n = 4 plants for WT, n = 5 plants for *rbohD rbohF*. *(B)* Relative stomatal conductances of WT and *rbohD/rbohF* double mutant whole rosette leaves. n = 5 plants for WT, n = 9 plants for *rbohD/rbohF*. Data represent mean ± SEM. *(C)* Genotyping of *rbohD/rbohF* double mutant. D211, D92b, F171, and F212 are gene specific primers described previously (8) and dSpm11 and dSpm1 are primers for the transposon insertion (9). D211: 5'-GTCGCCAAAGGAGGCGCCGA-3'; D92b: 5'-GGATACTGATCATAGGCGTGGCTCCA-3'; F171: 5'-CTTCCGATATCCTTCAACCAACTC-3'; F212: 5'-CGAAGAAGATCTGGAGACGAGA-3'; dSpm11: 5'-GGTGCAGCAAAACCCACACTTTTACTTC-3'; dSpm1: 5'-CTTATTTCAGTAAGAGTGTGGGGTTTTGG-3'. GeneRuler 1kb DNA ladder (Thermo Fisher Scientific Inc.) was loaded as DNA marker.

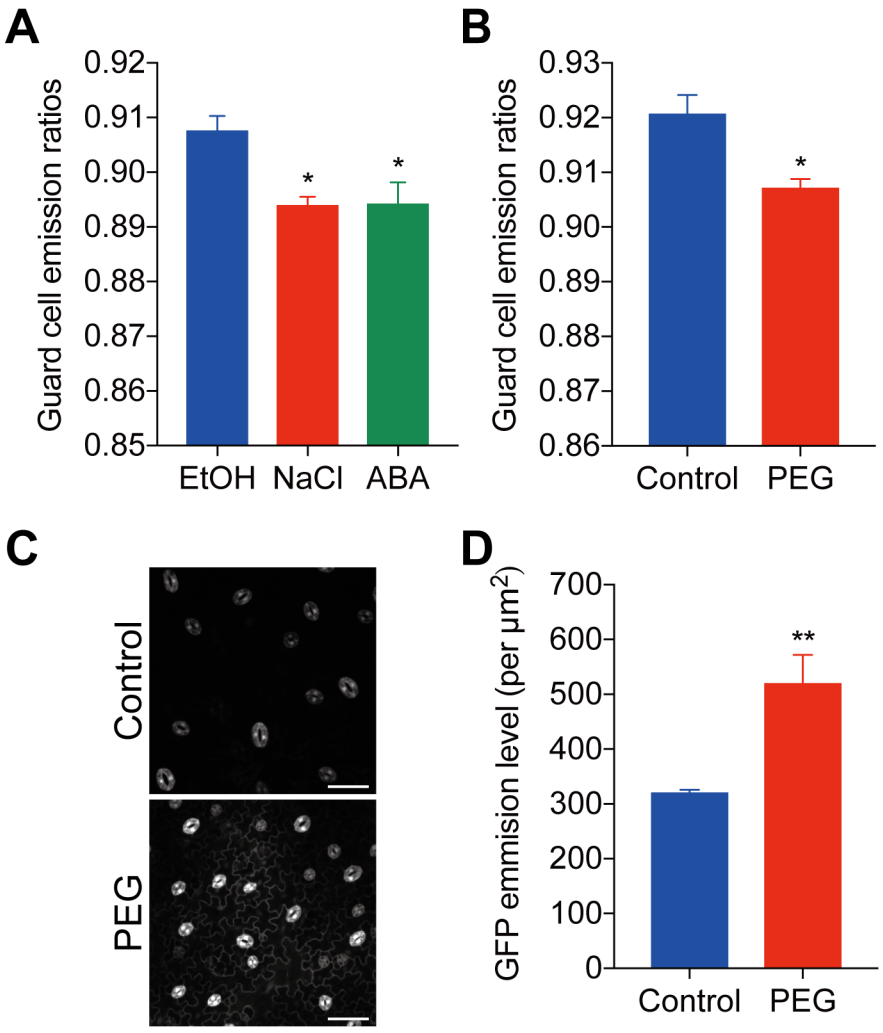

Fig. S8. Ratiometric ABAleon2.15 fluorescence changes in guard cells upon salt, low water potential and ABA treatments, and GFP expression driven by *RAB18* promoter in response to low water potential.

(A) ABAleon2.15 emission ratios (535/480 nm) in guard cells from seedlings treated with 140 mM NaCl, 20 µM ABA, or 0.02% EtOH treatment as control for 4 hrs. Data represent mean ± SEM. n = 3 experiments for each treatment with at least 30 guard cell pairs per experiment. * $P < 0.05$ as analyzed by one-way ANOVA followed by a Dunnett's test compared to WT control (B to D) Response of *pGC1::ABAleon2.15* or *pRAB18::GFP* seedlings to media in different water potential (Control = -0.31, PEG = -0.76 MPa). (B) ABAleon2.15 emission ratios in guard cells upon 4 hr treatment. Data represent mean ± SEM. n = 4 experiments for each treatment with at least 30 guard cell pairs per experiment. (C) Representative images of *pRAB18::GFP* promoter reporter expression in abaxial epidermes in response to the indicated treatments for 9 hrs. *(D)* Average *pRAB18::GFP* promoter reporter emission intensities in abaxial epidermes in *C*. GFP intensities were calculated by averaging 6 images of 3rd youngest leaves. Scale bar = 50 µm. Data represent mean ± SEM. n = 6 plants for each treatment. * $P < 0.05$, ** $P < 0.01$ by Student *t*-test in *B* and *D*.

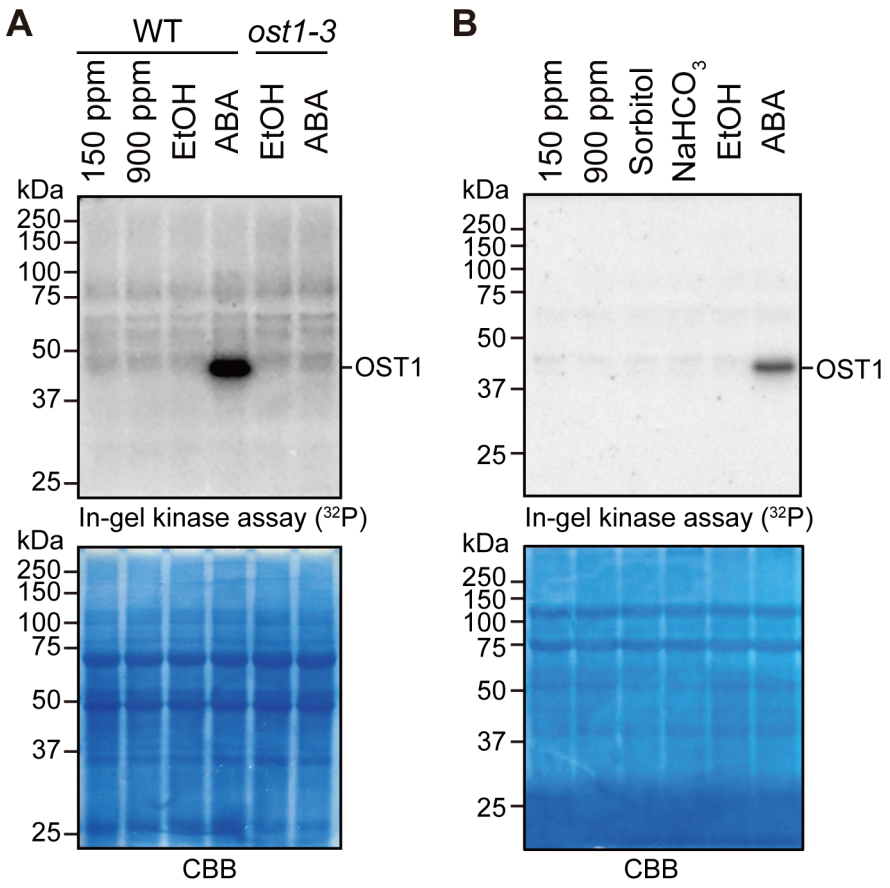

Fig. S9. Effect of CO_2 concentration on OST1/SnRK2 protein kinase activity in guard cells.

(A and B) In-gel kinase assays show ABA-activated OST1/SnRK2 protein kinase activity in guard cells. Col-0 (WT) and *ost1-3* guard cell protoplasts were exposed to CO_2-equilibrated buffer (150 or 900 ppm CO_2), 13.5 mM $NaHCO_3$ or 10 μM ABA for 30 min at room temperature. 27 mM sorbitol and 0.25% EtOH are controls for $NaHCO_3$ and ABA exposures, respectively. CBB staining is shown as a loading control.

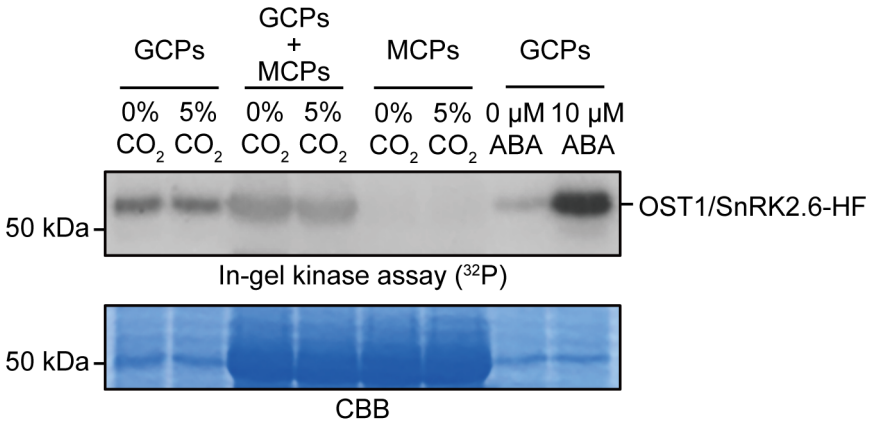

Fig. S10. Guard cell OST1/SnRK2.6 kinase activity is not affected by the presence of mesophyll cells in response to high CO_2.
In-gel kinase assay shows OST1/SnRK2.6-HF kinase activity in guard cells. Guard cell protoplasts (GCPs) were isolated from transgenic *ost1-3* knockout mutants carrying *pUBQ10::OST1/SnRK2.6-HF* (predicted M.W. ≈ 49 kDa) (7). Mesophyll cell protoplasts (MCPs) were prepared from Col-0 wild-type plants. Protoplasts were incubated in CO_2-equilibrated buffer, which had been aerated with 0 or 5% CO_2 containing air in advance at room temperature. GCPs were treated with 10 µM ABA or 0.25% EtOH (0 µM ABA) for 15 min in normal reaction buffer. The mobility of ABA-induced protein kinase was smaller than its expected value in SDS-PAGE. CBB staining is shown as a loading control for each set of experiments. Data represent one of three independent sets of experiments showing similar results.

Reference

1. Liu N, Ding Y, Fromm M, & Avramova Z (2014) Endogenous ABA Extraction and Measurement from *Arabidopsis* Leaves. *Bio Protoc* 4(19).
2. Azoulay-Shemer T*, et al.* (2015) Guard cell photosynthesis is critical for stomatal turgor production, yet does not directly mediate CO_2 - and ABA-induced stomatal closing. *Plant J* 83(4):567-581.
3. Schindelin J*, et al.* (2012) Fiji: an open-source platform for biological-image analysis. *Nat Methods* 9(7):676-682.
4. Verslues PE, Agarwal M, Katiyar-Agarwal S, Zhu J, & Zhu JK (2006) Methods and concepts in quantifying resistance to drought, salt and freezing, abiotic stresses that affect plant water status. *Plant J* 45(4):523-539.
5. Waadt R*, et al.* (2014) FRET-based reporters for the direct visualization of abscisic acid concentration changes and distribution in Arabidopsis. *eLIFE* 3:e01739.
6. Wu FH*, et al.* (2009) Tape-*Arabidopsis* Sandwich - a simpler *Arabidopsis* protoplast isolation method. *Plant Methods* 5:16.
7. Waadt R*, et al.* (2015) Identification of Open Stomata1-Interacting Proteins Reveals Interactions with Sucrose Non-fermenting1-Related Protein Kinases2 and with Type 2A Protein Phosphatases That Function in Abscisic Acid Responses. *Plant Physiol* 169(1):760-779.
8. Siddique S*, et al.* (2014) Parasitic worms stimulate host NADPH oxidases to produce reactive oxygen species that limit plant cell death and promote infection. *Sci Signal* 7(320):ra33.
9. Tissier AF*, et al.* (1999) Multiple independent defective *Suppressor-mutator* transposon insertions in Arabidopsis: a tool for functional genomics. *Plant Cell* 11(10):1841-1852.